

# Initial Scaling on Metal Surfaces at Binary Geothermal Plant of Obama Hot Spring in Japan

Motoaki Morita and Shinichi Motoda

Tokyo University of Marine Science and Technology, 2-1-6 Etchujima, Koto-ku, Tokyo, 135-8533 Japan

E-mail morita@kaiyodai.ac.jp

**Keywords:** Layered silicate, Magnesium silicate, Calcium carbonate, Heat exchanger, Transport pipe

## ABSTRACT

Microstructures of scales adhered on a steel transportation pipe of geothermal fluid and a plate for a heat exchanger collected from a geothermal plant in Obama town, Unzen city, Nagasaki, Japan were analyzed by SEM-EDS and XRD. There were three locations where scales were sampled: a steel pipe for a transportation of geothermal fluid before aeration and decarboxylation, a steel pipe after the aeration and decarboxylation, and a titanium plate used at heat exchanger. By observation from cross section, the mineral phases of the main scales, that of the initial scales, and the nucleation sites of the initial scale in their scales were investigated. Calcium carbonate was the mineral phase of the main scale adhered on a steel pipe for transportation of geothermal fluid before aeration and decarboxylation. Magnesium silicate was the mineral phase of the main scale on the other locations. The mineral phases of the initial scales at all locations were magnesium silicate. Corrosion product seems to be preferred site for scaling steel pipes because corrosion product of iron is covered with magnesium silicate. On the other hand, the nucleation site of magnesium silicate adhered on a titanium plate was not identified. The XRD patterns for their initial scales exhibited the layered magnesium silicate with low crystallinity. Their patterns were not corresponding to those of typical layered magnesium silicates (e.g. talc and sepiolite). It is possible that scaling at the system utilizing the geothermal fluid at Obama town becomes slow by preventing precipitation of layered magnesium silicate which is the mineral phase of the initial scale.

## 1. INTRODUCTION

At Obama town which is located on the foothills of the Mt. Unzen volcano, the gushing of the hot spring water around 100 °C with the production rate 15,000 ton/day is well known. People of Obama town has been trying to utilize the huge heat capacity from hot spring water. One of the utilization methods is the small power generation by binary cycle power generation system (Figure 1). The system is comprised of three units: hot spring water unit, binary power generation unit, and cooling water unit. Since hot spring water generally exhibits scaling property, a primary heat exchanger that can be disassembled is usually arranged for facilitate maintenance. However, hot spring water at Obama town has very high scaling property, and intervals for maintenance of transportation pipe and heat exchanger are only once in three months, and the intervals are once in three weeks in the case of hot spring water without controlling the water quality. Chemical injection is expected to one of suppression method for scaling, but there is a demand for scale countermeasures that are more environmentally benign in Japan. To develop a novel chemical with few environmental harm, and a novel material with anti-scaling property, the microstructure of scale formed on the materials is needed to be understood. In this paper, the microstructures of scales formed on the steel pipe and titanium plate of heat exchanger in hot spring water at Obama town were analyzed. Then, the effect of aeration and decarboxylation on the microstructure of scale were investigated. Finally, mineral phases of the main scale, the initial scale, and the nucleation site of the initial scales were summarized.

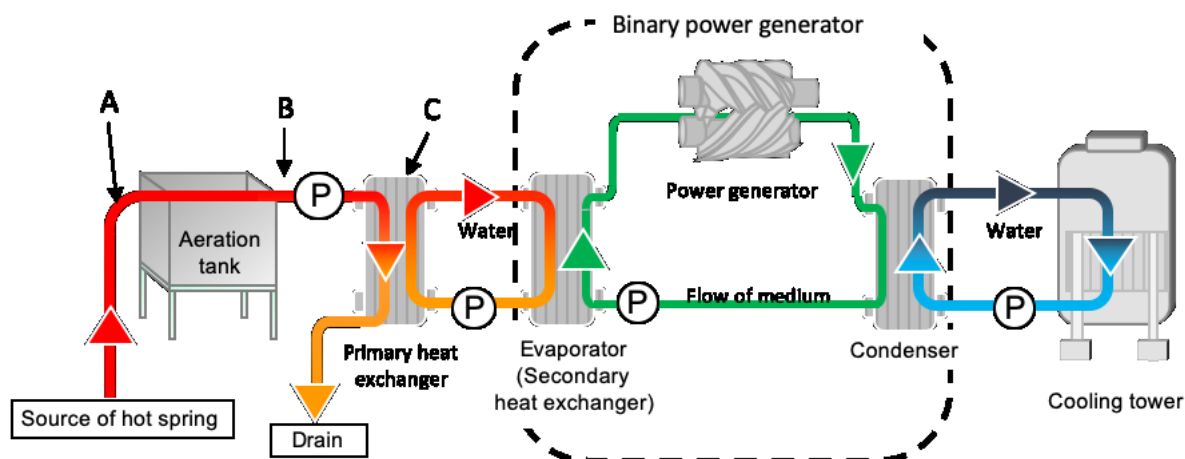


Figure 1: System diagram of binary cycle power generation system for hot spring water in this study (Takahashi et al. (2013)). Sampling locations A, B, and C in this study are shown in this figure.

## 2. EXPERIMENT

### 2.1 Samples

Two steel pipes to transport geothermal fluid at the binary power plant of Obama hot spring from April 1 to July 17, 2013 were sampled. One steel pipe was sampled from location A before the tank for aeration and decarboxylation as shown in figure 1. Another pipe was sampled from location B, where the geothermal fluid flows in after the tank. Titanium plate for heat exchanger at location C was used for 3 weeks under its operation. Steel pipes are an ASTM A53, and titanium plate was an ASTM B265 Gr. 2. Their samples were cut from the pipes and the plate and embedded to the resin as shown in figure 2. Chemical composition of geothermal fluid (102°C) is shown in Table 1. Calcium carbonate and amorphous magnesium silicate are supersaturation in this geothermal fluid (Morita et al. (2017)).

### 2.2 Microstructural analyses

Optical microscopy and FE-SEM (field-emission scanning electron microscopy) with an EDS (energy-dispersive spectroscopy) detector were used to characterize the microstructures of the scales adhered on the pipes and the plate. The randomly oriented samples of the initial and the main scales formed on them were prepared, their mineral phases were identified by the X-ray diffraction (XRD). Knife edge was equipped to XRD to achieve a reduction in scattering on the low-angle side.

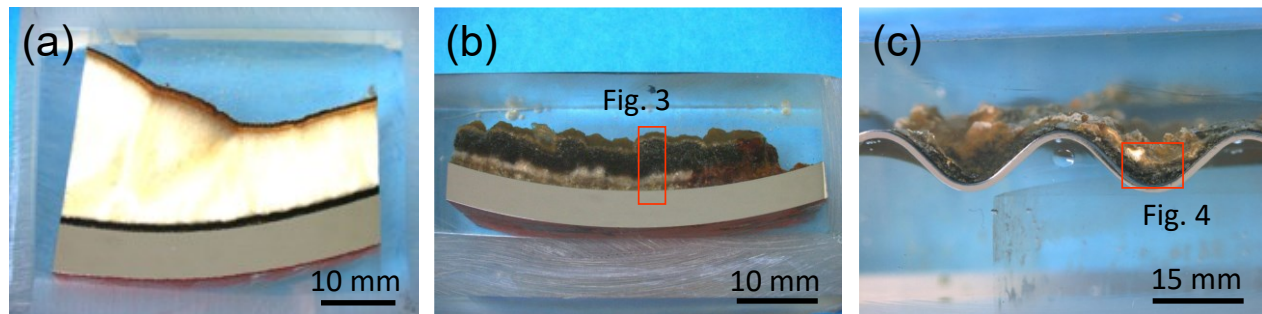


Figure 2: Optical photographs of samples: (a) pipe at location A shown in figure 1 (Morita and Umezawa (2016)), (b) pipe at location B, and (c) titanium plate at location C.

Table 1 Chemical composition of hot spring water and gas in steam at Obama marina source (Morita et al. (2017)).

Element	Water													Gas in steam			
	pH	Na	K <sup>+</sup>	Ca <sup>2+</sup>	Mg <sup>2+</sup>	Cl <sup>-</sup>	SO <sub>4</sub> <sup>2-</sup>	Al <sup>3+</sup>	HCO <sub>3</sub> <sup>-</sup>	F <sup>-</sup>	B <sup>3+</sup>	As <sup>5+</sup>	Total-SiO <sub>2</sub>	Water-gas ratio	CO <sub>2</sub>	H <sub>2</sub> S	R gas
Unit	—	ppm	ppm	ppm	ppm	ppm	ppm	ppm	ppm	ppm	ppm	ppm	ppm	(volume ratio)	vol%	vol%	vol%
Amount	8.2	2510	290	134	128	4530	297	<0.01	166	0.53	15.2	0.42	223	1.39	97.3	0.4	2.3

## 3. RESULTS AND DISCUSSION

### 3.1 Scaling on steel pipe for transportation of geothermal fluid before aeration and decarboxylation

In previous study (Morita and Umezawa (2016)), the microstructure of scales adhered on a steel pipe for transportation of geothermal fluid before aeration and decarboxylation was analyzed. The scales had four layers, and the first, second, third, and fourth mineral phases layers from the inner surface of the pipe were the corrosion product of the carbon steel, amorphous-like magnesium silicate, calcium carbonate, and amorphous-like magnesium silicate, respectively. The mineral phase of the initial scale was amorphous-like magnesium silicate, and then calcium carbonate adhered on amorphous-like magnesium silicate. Calcium carbonate seems to grow from amorphous-like magnesium silicate which is the initial scale. On the other hand, the nucleation site of amorphous-like magnesium silicate was on the corrosion product. The Mg/Si ratio of the magnesium silicate at the initial scale was 0.4–0.42.

### 3.2 Scaling on steel pipe for transportation of geothermal fluid after aeration and decarboxylation

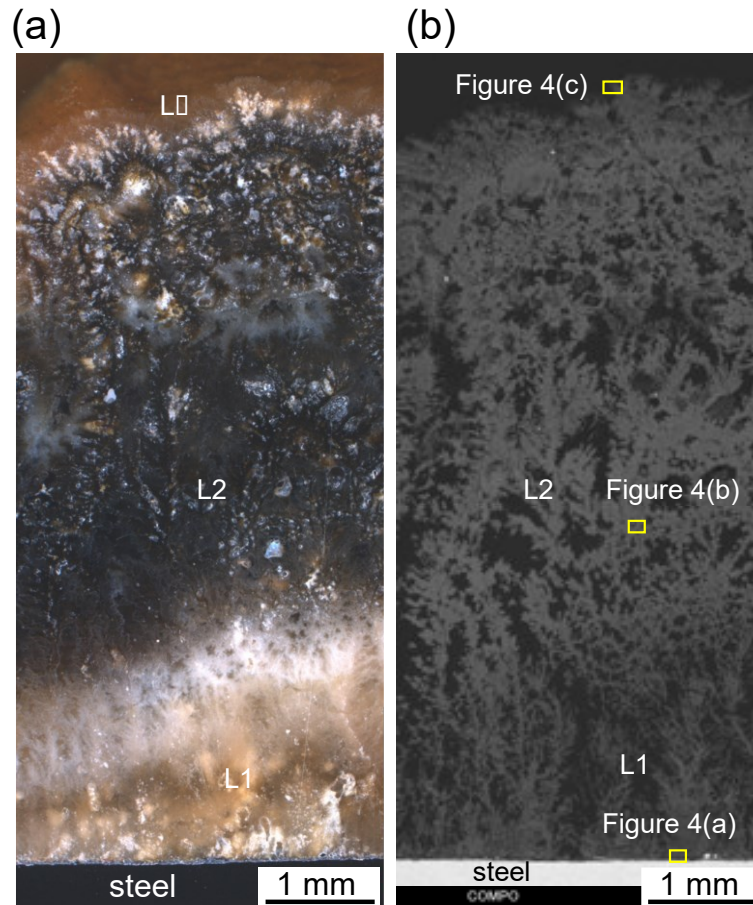
#### 3.2.1 Macrostructure of scales

Figure 3 (a) shows a magnified optical photograph of the image shown in figure 2(b). After aeration and decarboxylation, the scales had a poorly layered structure. There were three layers which are denoted by different colors from the inner wall of the steel pipe: a cream-colored layer (L1), a black layer (L2), and a cream-colored layer (L3). Figure 3(b) shows a backscattered electron (BSE) image of the same region with Figure 3(a). In all BSE images, a darkest contrast region shows a resin for embedding sample. The contrast of L1 layer is almost the same with that of L2, and gaps do not exist among L1 layer, L2 layer, and L3 layer. The composition of all the layers seems to be similar to each other. A morphology exhibited dendrite structure and porosity.

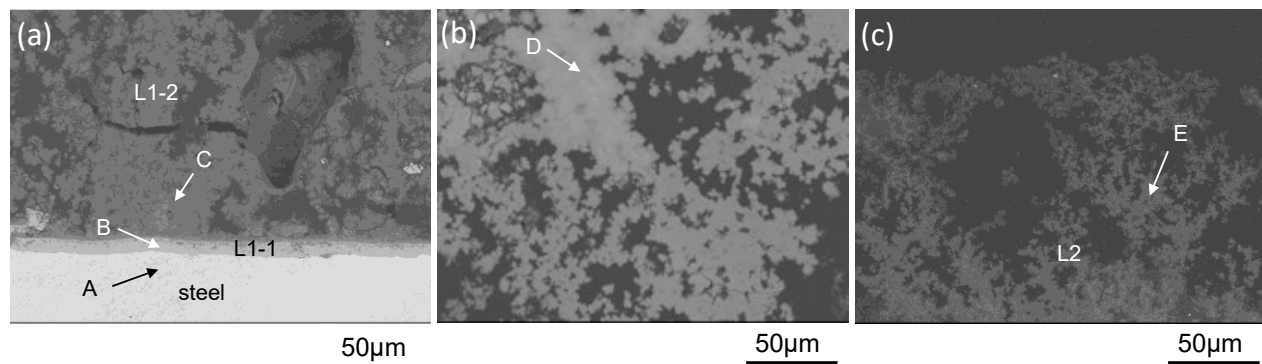
#### 3.2.2 Microstructure of scales

Figure 4 shows a magnified version of the image shown in Figure 3(b). The inner region of L1 layer consists of two types of scales (Figure 4(a)). The gray part adhering to the carbon steel surface is labeled as L1-1 layer, and the black part is labeled as L1-2 layer. Gaps do not exist between L1-1 layer and L1-2 layer, and L1-2 layer is totally covered with L1-1. L1-1 layer is the nucleation site of the scale at L1-2. Table 2 shows the chemical compositions at the points A to E shown in figure. 4. Concentration of carbon element is removed from this tables because of the low accuracy for carbon. The detected elements at the analysis point A are only

iron and carbon. The L1-1 layer (analysis point B) on the substrate is comprised of Fe and O. L1-1 layer is the corrosion product. A corrosion product firstly adhered on a steel pipe. L1-2 layer (analysis point C), L2 layer (analysis point D), and L3 layer (analysis point E) comprised primarily Si, Mg, and O. The concentration of Ca is low. Their chemical compositions were also very similar to each other. The L1-2, L2, and L3 are magnesium silicate, and their Mg/Si ratio were 0.58~ 0.77. A difference of color among the layers does not result from the chemical composition, and analysis of chemical bonding state is needed in the future to make it clear. Based on the above results, a corrosion product firstly produces on the inner steel pipes not only before aeration and decarboxylation but also after them, and then magnesium silicate seems to start scaling.



**Figure 3: Scales formed at a steel pipe used for the transportation of geothermal fluid after aeration and decarboxylation: (a) optical photograph and (b) backscattered electron image.**



**Figure 4: Magnified images of figure 3(b)**

**Table 2: Chemical compositions of points A~E shown in figure 4.**

Point	O	Mg	Si	Ca	Fe
A	0.0	0.0	0.0	0.0	100.0
B	58.7	0.0	0.0	0.0	41.5
C	60.5	16.4	21.3	0.4	1.3
D	55.2	16.9	26.1	0.7	1.1
E	50.9	16.8	28.7	1.7	1.8

### 3.3. Scaling on the titanium plate used for heat exchanger of geothermal fluid after aeration and decarboxylation

#### 3.3.1 Macrostructure of scales

Figure 5(a) shows a magnified optical photograph of the image shown in figure 2(c). The temperature of hot spring water at input side and that of at outlet side were 98 °C and 74.5 °C, respectively. Two areas were divided from scales by the difference of color: a black color area (Ar1 and Ar2) and a white color area (Ar3). Contrasts at Ar1, Ar2, and Ar3 in BSE image were almost the same with each other, and scales at their areas seem to have similar chemical compositions. Macro structure of scale exhibited denser compared to the pipe under the same condition.

#### 3.3.2 Microstructure of scales

The initial scale directly adhered on the titanium plate in the observation area (figure 6(a)). Areas with a white color in BSE image can be partially confirmed (e.g. Ar2 shown in figure 6(b)). Elements of Fe and S were detected at the area with white color (Point D shown in table 3), and its mineral phase seems to be iron sulfide. Ar1 (Point B), Ar2 (Point D), and Ar3 (Points E and F) with contrast of grey color comprised primarily O, Mg, and Si, and minute amounts of Fe, Ca, and Mn are also present. The mineral phase of the main scale was magnesium silicate, and Mg/Si ratio was 0.61~0.75. The Mg/Si ratio was similar to the scale on the steel pipe for transportation of geothermal fluid after aeration and decarboxylation. Even if corrosion product of iron is none, magnesium silicate directly adheres on a material. Scales with dense structure and porous structure were mixed at Ar3, but their chemical compositions were similar to each other. Chemical composition does not affect the macro structure of scale.

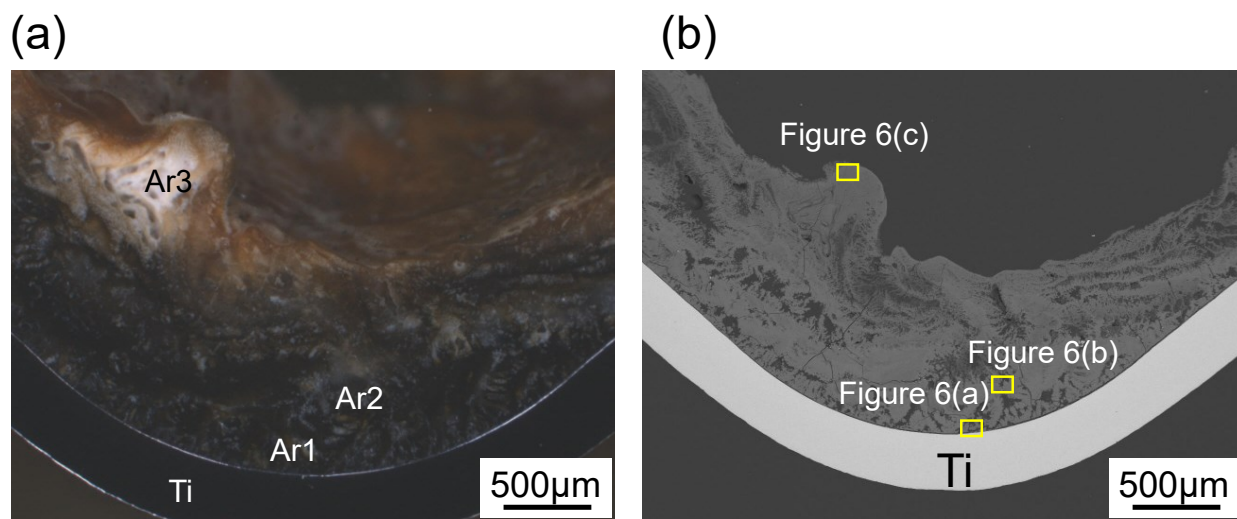


**Figure 5: (a) Scales formed at the titanium plate used for heat exchanger of geothermal fluid after aeration and decarboxylation: (a) optical photograph and (b) backscattered electron image.**

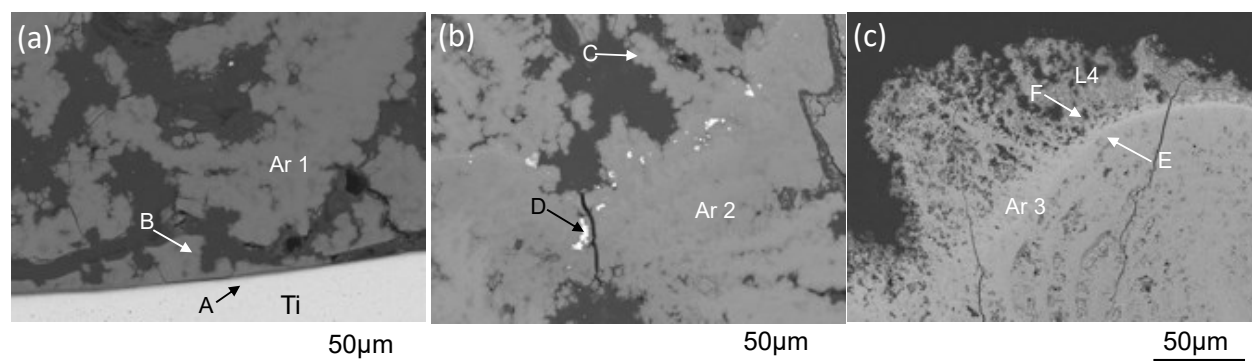


Figure 6: Magnified images of figure 5 (b).

Table 3: Chemical compositions of points A~F shown in figure 6.

Point	O	Mg	Si	Ca	Fe	S	Mn	Ti
A	—	—	—	—	—	—	—	100.0
B	63.2	13.3	20.6	—	2.4	0.0	0.8	—
C	62.3	11.5	18.8	0.3	0.6	—	0.6	—
D	—	—	1.6	—	32.2	66.4	—	—
E	58.1	17.2	22.9	—	1.2	—	0.8	—
F	58.4	15.8	22.4	—	2.2	—	1.1	—

### 3.4. XRD analysis

Figure 7 shows XRD patterns of the initial scales formed at a steel pipe for transportation of geothermal fluid before and after aeration and decarboxylation, and the titanium plate for heat exchanger. The reflection peaks of the initial scale formed on the steel pipe for transportation of geothermal fluid before aeration and decarboxylation are indistinct. On the other hand, some reflection peaks on a steel pipe and a titanium plate were detected. The reflection peaks were similar to those of the representative layered magnesium silicates: talc and sepiolite. The first reflection peak of talc  $d(001)$  (Perdikatsis et al. (1981)) and that of sepiolite  $d(101)$  (Hayashi (1969); Yoniyol (2014)) are observed at  $2\theta = 9.5^\circ$  and  $7.3^\circ$ , respectively. The first reflection peaks of the initial scales formed at the steel pipe for the transportation of geothermal fluid before and after aeration and decarboxylation, and the peak at titanium plate of heat exchanger were  $2\theta = 7.9^\circ$ ,  $6.1^\circ$ , and  $6.6^\circ$ , respectively. The peaks of the samples corresponded the peaks of sepiolite. The other peaks also corresponded the peaks of sepiolite which were reported in the crystallized sepiolite (Brauner and Preisinger (1996)). However, some reflection peaks were not detected. Especially, the initial scales before aeration and decarboxylation had few peaks. In addition,  $(hk0)$  peaks seems to be sufficiently detected. It may indicate that the crystal structure disordered along  $c$ -axis. Hydrated magnesium silicate (M-S-H), which cannot be straightforwardly related to typical magnesium silicate minerals (Zhang et al. (2014)), is also similar to the reflection peaks after the second peak of the initial scales. Though M-S-H has no reflection peak below  $2\theta = 10^\circ$ , and the peaks of M-S-H roughly corresponded to those of the initial scales. In the scales after aeration and decarboxylation, a broad peak can be detected around  $2\theta=25^\circ$ . Zhang et al. (2014) pointed out that the broad peak would be derived from  $\text{SiO}_2$ . On the other hand, crystalline sepiolite has three reflection peaks of  $d(400)$ ,  $d(241)$ , and  $d(080)$  (Brauner and Preisinger (1996)). Thus, it was difficult to identify a mineral phase with the broad peak around  $2\theta=25^\circ$ . To identify the mineral phase and the crystal structure of the initial scales at the Obama hot spring, more detailed analyses is needed in the future.



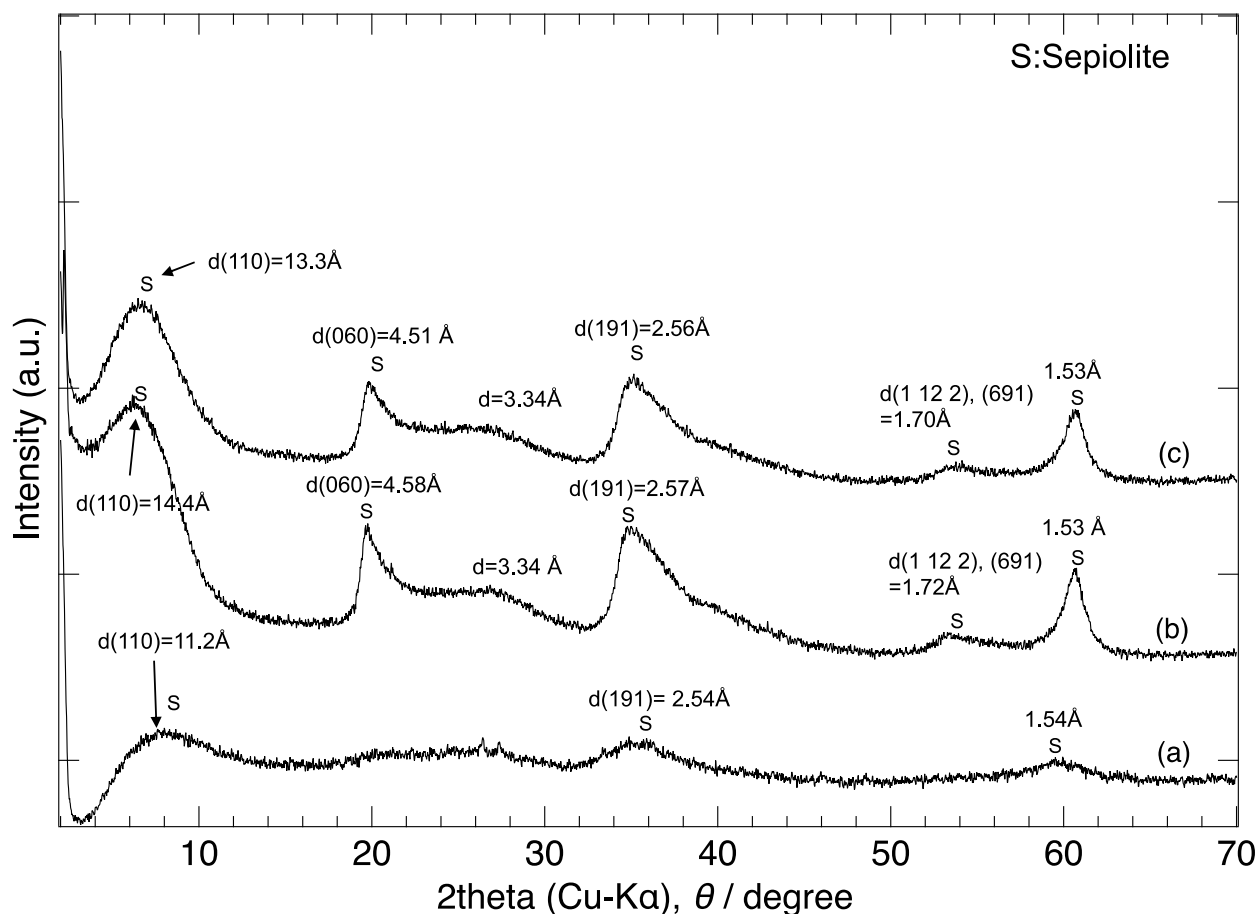


Figure 7: XRD diffractograms of the randomly oriented initial scales at (a) location A, (b) location B, and (c) location C.

### 3.5 Main scale and initial scale at Obama town

The main scales formed at a steel pipe for transportation of geothermal fluid before and after aeration and decarboxylation, and the titanium plate of heat exchanger were calcium carbonate, magnesium silicate, and magnesium silicate, respectively (Table 4). Treatments of aeration and decarboxylation inhibit a precipitation of calcium carbonate. Since grain growth rate of calcium carbonate is rapid (Morita and Umezawa (2016)), and scaling rate becomes low under geothermal fluid after acceleration of decarboxylation (figure 1(a) and (b)). The initial scales at Obama town are magnesium silicate with poorly layered structure. To prevent the scaling effectively in hot spring water at Obama town, the precipitation of magnesium silicate should be inhibited. In a steel pipe, the nucleation sites of the magnesium silicate were corrosion product of iron. Daniela et al. (2016) reported that corrosion of carbon steel was prevented under the environment where silica scaling is high. This study suggests that preferred location for scaling is on corrosion product, and as the result, silica scale may prevent to progress corrosion. Magnesium silicate adhered on titanium without corrosion product.

Table 4: Summarization of the main scale, the initial scale, and the nucleation site of initial scale formed on materials for transportation and heat exchange of geothermal fluid at Obama town.

Location shown in figure 1	Condition				Scale		
	Material	Fluid state	Aeration and decarboxylation treatments		Mineral phase of main scale	Mineral phase of initial scale	Nucleation site of initial scale
Location A	Carbon steel pipe	Liquid and gas	—	=>	CaCO <sub>3</sub>	Mg silicate	Corrosion product of Fe
Location B	Carbon steel pipe	Liquid	○	=>	Mg silicate	Mg silicate	Corrosion product of Fe
Location C	Titanium plate	Liquid	○	=>	Mg silicate	Mg silicate	(Unidentified)

## 4. CONCLUSIONS

Microstructures of scales formed at a small geothermal plant utilizing extra hot spring water at Obama town, Nagasaki pref., Japan were analyzed. Then, mineral phases of main scales, those of initial scales, and nucleation site of initial scale were investigated. The following conclusions were obtained by the above experiments.

- (1) By aeration and decarboxylation treatments, main scales changed from calcium carbonate to magnesium silicate.

- (2) Mineral phases of initial scales at all locations were the same, and the mineral phases were magnesium silicate with low crystallinity.
- (3) Corrosion product was fully covered with magnesium silicate. Corrosion product is preferred site for scaling.
- (4) It is possible that scaling at the system utilizing the geothermal fluid at Obama town is inhibited by preventing a precipitation of magnesium silicate which is an initial scale.

## ACKNOWLEDGMENT

Parts of these findings were the results of the project “geothermal power generation technology research and development” commissioned by the New Energy and Industrial Technology Development Organization (NEDO). Part of this work was supported by the JSPS KAKENHI Grant Number 19H02453. The field study was performed with the cooperation of the Obama Onsen Energy and the Edit Inc.. We would like to express our sincere gratitude to them.

## REFERENCES

- Brauner, K. and Preisinger, A.: Struktur und Entstehung des Sepioliths, *Tschermaks mineralogische und petrographische Mitteilungen*, **6**, (1956), 120-140.
- Heuvel, D.B., Gunnlaugsson, E., Benning, L.G.: Passivation of metal surfaces against corrosion by silica scaling, *Proceedings of 41<sup>st</sup> Workshop on Geothermal Reservoir Engineering*, (2016), 1-10.
- Hayashi, H.: Infrared study of sepiolite and palygorskite on heating, *The American Mineralogist*, **53**, (1969), 1613-1624.
- Morita, M. and Umezawa, O.: A model of scale formation on inner steel pipe for transporting hot spring water, *Materials Transactions*, **57**, (2016), 1652-1659.
- Morita, M., Goto, Y., Motoda, S., and Fujino, T.: Thermodynamic Analysis of Silica-Based Scale Precipitation Induced by Magnesium Ion, *Journal of the Geothermal Research Society of Japan*, **39**, (2017), 191-201.
- Perdikatsis, B., and Burzlaff, H.: Strukturverfeinerung am Talk  $Mg_3[(OH)_2Si_4O_{10}]$ , *Zeitschrift für Kristallographie - Crystalline Materials*, **156**, (1981), 177-186.
- Takahashi, K., Matsuda, H., Fujisawa, R., Matsumura M., Narukawa, Y., and Adachi, S.: Binary Cycle Power Generation System for Hot Water, *Kobe Steel Engineering Reports*, **63**, (2013), 2-5. (in Japanese)
- Yoniyol, M.: Characterization of two forms of sepiolite and related Mg-rich clay minerals from Yenidoğan (Sirvihisar, Turkey), *Clay Minerals*, **49**, (2014), 91-108.
- Zhang, T., Vandeperre, L., and Cheeseman, C.R.: Formation of magnesium silicate hydrate (M-S-H) cement pastes using sodium hexametaphosphate, *Cement and Concrete Research*, **65**, (2014), 8-14.